ANALYTICAL AND NUMERICAL ANALYSIS OF BONDED JOINTS AND REINFORCEMENTS BY DOUBLERS IN AERONAUTICAL STRUCTURES

Fanton, F., ffanton@fem.unicamp.br
Rodriguez, R.Q, reneqr87@fem.unicamp.br
Sollero, P, sollero@fem.unicamp.br
Rodrigues, M.R.B., marcelo.bertoni@embraer.com.br
Faculty Mechanical Engineering, State University of Campinas, 13083-970, Campinas, Brazil

Albuquerque, E. L, eder@unb.br
Faculty of Technology, University of Brasilia, 70910-900, Brasília, Brasil

Abstract. *The development of new materials and processes is followed by considerable advances in structural design. Optimized design of structures frequently requires the usage of different materials together, materials that cannot be welded or structures in which bolted or riveted connections are not admitted. As an alternative, the application of adhesives in bonded joints is increasing. Bonded joints have been studied extensively for the last six decades with many analytical work focused on the study of adhesive stress. This paper presents a software developed in Matlab for stress calculation, using the models available in literature: Volkersen, Goland & Reissner, Hart-Smith & Eidinoff and Ojalvo. Results were compared through Matlab and numerical models developed in the commercial software ABAQUS. Summarizing, this paper aims to study bonded joints in aircraft structures, through analytical and numerical analysis. Having a special focus on areas of stress concentration such as doors edges, windows, wings and crack repairs, where reinforcements should be located. In this study was used reinforcements by doublers (additional plates attached to a base plate by an adhesive film). Doublers have the advantage of efficient load transfer, low cost use, high corrosion and fatigue resistance, and the reduction of the relation "buy to fly", that is the relationship between the weight of the material purchased and the weight of the material that is effectively in the product.*

Keywords*: Bonded joints, adhesives, analytical methods, single lap joints, doublers*

1. INTRODUCTION

Structures frequently require the usage of different materials together, materials that cannot be welded or in which bolted or riveted connections are not admitted. As an alternative, the application of adhesives in bonded joints is increasing. When compared with others methods of union, bonded joints present many advantages as: ability to conform strong light weight structures, uniform stress distribution along the overlap with no stress concentration, enhanced fatigue properties, improved corrosion resistance, smoother surfaces, among others. The most common joint type is the Single Lap Joint (SLJ). Volkersen, Goland & Reissner, Hart-Smith & Eidinoff and Ojalvo where pioneers in the study of the stress distribution in SLJ's. Also were developed essential formulations for the analysis of doublers, these models were developed recently by Hart-Smith (2004) and C.N. Duong (2006). Doublers are plates attached to a base plate by an adhesive film. Doublers have the advantage of efficient load transfer, low cost use, high corrosion and fatigue resistance, and the reduction of the relation "buy to fly", that is the relationship between the weight of the material purchased and the weight of the material that is effectively in the product. This paper aims to study bonded joints in aircraft structures, through analytical and numerical analysis. Having a special focus on areas of stress concentration such as doors edges, windows, wings and crack repairs, where reinforcements should be located. A brief description of each method is shown in the first part of this paper. Then, a comparison between these methods and finite element analysis is shown.

2. ANALYTICAL MODELS

2.1. SINGLE LAP JOINTS (SLJ)

2.1.1. VOLKERSEN

The first analytical method known in literature for the stress analysis of bonded joints was developed by (Volkersen, 1938). Volkersen method, also known as the "shear-lag model", introduced the concept of differential shear. The bending effect caused by the eccentric load path is not considered. The adhesive shear stress distribution τ is given by:

$$\tau = \frac{P\omega}{2b}\cdot\frac{\cosh(\omega x)}{\sinh\left(\frac{\omega l}{2}\right)} + \left(\frac{t_t - t_b}{t_t + t_b}\right)\cdot\left(\frac{\omega l}{2}\right)\cdot\frac{\sinh(\omega x)}{\cosh\left(\frac{\omega l}{2}\right)} \tag{1}$$

where

$$\omega = \sqrt{\frac{G_a}{E t_t t_a}\left(1 + \frac{t_t}{t_b}\right)}$$

and t_t is the top adherend thickness, t_b is the bottom adherend thickness, t_a is the adhesive thickness, b is the bonded area width, l is the bonded area length, E is the adherend modulus, G_a is the adhesive shear modulus and *P* is the force applied to the inner adherend. The origin of x is the middle of the overlap.

2.1.2. GOLAND & REISSNER

(Goland & Reissner, 1944) were the first to consider the effects due to rotation of the adherends. They divided the problem into two parts: (a) determination of the loads at the edges of the joints, using the finite deflection theory of cylindrically bent plates and (b) determination of joint stresses due to the applied loads. The adhesive shear stress distribution τ found by Goland & Reissner is given by:

$$\tau = -\frac{1}{8}\frac{\overline{P}}{c}\left\{\frac{\beta c}{t}(1+3k)\frac{\cosh\left(\frac{\beta c}{t}\frac{x}{c}\right)}{\sinh(\beta c/t)} + 3(1-k)\right\} \tag{2}$$

where, $\overline{P}$ is the applied tensile load per unit width, c is half of the overlap length, t is the adherend thickness and k is the bending moment factor given by (Goland & Reissner, 1944):

$$k = \frac{\cosh(u_2 c)}{\cosh(u_2 c) + 2\sqrt{2}\sinh(u_2 c)}$$

where $u_2 = \sqrt{\frac{3(1-\nu^2)}{2}}\frac{1}{t}\sqrt{\frac{\overline{P}}{tE}}$; $\beta^2 = 8\frac{G_a}{E}\frac{t}{t_a}$ and ν is Poisson's ratio.

The adhesive peel stress distribution σ is given by:

$$\begin{aligned}\sigma = \frac{1}{\Delta}\frac{\overline{P}t}{c^2}\Bigg[&\left(R_2\lambda^2\frac{k}{2} + \lambda k'\cosh(\lambda)\cos(\lambda)\right)\cosh\left(\frac{\lambda x}{c}\right)\cos\left(\frac{\lambda x}{c}\right) \\ &+\left(R_1\lambda^2\frac{k}{2} + \lambda k'\sinh(\lambda)\sin(\lambda)\right)\sinh\left(\frac{\lambda x}{c}\right)\sin\left(\frac{\lambda x}{c}\right)\Bigg]\end{aligned} \tag{3}$$

where k' is the transverse force factor.

$$k' = \frac{kc}{t}\sqrt{3(1-\nu^2)\frac{\overline{P}}{tE}};\ \lambda = \gamma\frac{c}{t};\ \gamma^4 = 6\frac{E_a}{E}\frac{t}{t_a},\ \Delta = \frac{1}{2}(\sin(2\lambda) + \sinh(2\lambda))$$

$$R_1 = \cosh(\lambda)\sin(\lambda) + \sinh(\lambda)\cos(\lambda);\ R_2 = -\cosh(\lambda)\sin(\lambda) + \sinh(\lambda)\cos(\lambda)$$

2.1.3. HART-SMITH

In contrast with (Volkersen, 1938) or (Goland & Reissner, 1944), (Hart-Smith, 1973) considered adhesive plasticity. In the report presented for the NASA they analyzed both, the single lap joint (SLJ) and the double lap joint (DLJ). For both analyses they combined elastic peel stress with plastic shear stresses. According to Hart-Smith, the adhesive elastic shear stress distribution τ is given by:

$$\tau = A_2 \cosh(2\lambda' x) + C_2 \tag{4}$$

where,

$$\lambda' = \sqrt{\left[\frac{1+3(1-\nu^2)}{4}\right]\frac{2G_a}{t_a E t}};\ A_2 = \frac{G_a}{t_a E t}\left[\overline{P} + \frac{6(1-\nu^2)M}{t}\right]\frac{1}{2\lambda'\sinh(2\lambda' c)}$$

$$C_2 = \frac{1}{2c}\left[\overline{P} - \frac{A_2}{\lambda'}\sinh(2\lambda' c)\right];\ M = \overline{P}\left(\frac{t+t_a}{2}\right)\frac{1}{1+\xi c+\left(\frac{\xi^2 c^2}{6}\right)};\ \xi^2 = \frac{\overline{P}}{D}$$

and D is the adherend bending stiffness given by: $D = \dfrac{Et^3}{12(1-\nu^2)}$.

Variables $\overline{P}$, G_a, t_a, E, ν, t, c have the same meaning as presented by (Volkersen, 1938) and (Goland & Reissner, 1944) models. The adhesive peel stress distribution σ is given by:

$$\sigma = A\cosh(\chi x)\cos(\chi x) + B\sinh(\chi x)\sin(\chi x) \tag{5}$$

where, $\chi^4 = \dfrac{E_a}{2Dt_a}$; $A = -\dfrac{E_a M[\sin(\chi c) - \cos(\chi c)]}{t_a D\chi^2 e^{(\chi c)}}$; $B = \dfrac{E_a M[\sin(\chi c) + \cos(\chi c)]}{t_a D\chi^2 e^{(\chi c)}}$

and E_a is the Young modulus of the adhesive.

The shear plastic stress was modeled using a bi-linear elastic-perfectly plastic approximation. The overlap is divided into three regions, a central elastic region of length d and two outer plastic regions. Coordinate x' starts in the plastic region. The problem is solved in the elastic region in terms of the shear stress according to:

$$\tau = A_2 \cosh(2\lambda' x) + \tau_p(1-K) \tag{6}$$

and the shear strain in the plastic region according to:

$$\gamma = \gamma_e\left\{1 + 2K\left[(\lambda' x')^2 + \lambda' x'\tanh(\lambda' d)\right]\right\} \tag{7}$$

where τ_p is the plastic adhesive shear stress and $A_2 = \dfrac{K\tau_p}{\cosh(\lambda' d)}$.

K and d are solved by an iterative approach using the following equations:

$$\frac{\overline{P}}{l\tau_p}(\lambda' l) = 2\lambda'\left(\frac{l-d}{2}\right) + (1-K)(\lambda' d) + K\tanh(\lambda' d) \tag{8}$$

$$\left[1+3k(1-\nu^2)\left(1+\frac{t_a}{t}\right)\right]\frac{\overline{P}}{\tau_p}\lambda^2\left(\frac{l-d}{2}\right) = 2\left(\frac{\gamma_p}{\gamma_e}\right) + K\left[2\lambda'\left(\frac{l-d}{2}\right)\right]^2 \tag{9}$$

$$2\left(\frac{\gamma_p}{\gamma_e}\right) = K\left\{\left[2\lambda'\left(\frac{l-d}{2}\right) + \tanh(\lambda' d)\right]^2 - \tanh^2(\lambda' d)\right\} \tag{10}$$

where, γ_e and γ_p are the elastic and plastic adhesive shear strain respectively.

2.1.4. OJALVO & EIDINOFF

(Ojalvo & Eidinoff, 1978) model is based on (Goland & Reissner, 1944) model. They modified some coefficients in the shear stress equations by adding new terms in the differential equation and considering new boundary conditions for bond peel stress calculation. Their leading work was the first in predicting the variation of shear stress through the bond thickness. The adhesive nondimensional shear stress distribution τ^* found by (Ojalvo & Eidinoff, 1978) is given by:

$$\tau^* = A\cosh\left(\lambda\sqrt{2+6(1+\beta)^2}\,x^*\right) + B \tag{11}$$

where,

$$A = \frac{2\lambda\left(1+3(1+\beta)^2 k\right)}{\sqrt{2+6(1+\beta)^2}\sinh\left(\lambda\sqrt{2+6(1+\beta)^2}\,x^*\right)};\ B = 1 - \frac{A\sinh\left(\lambda\sqrt{2+6(1+\beta)^2}\right)}{\lambda\sqrt{2+6(1+\beta)^2}}$$

$$\lambda^2 = \frac{G_a c^2}{E^* t h};\ \beta = \frac{h}{t}$$

where $E^* = E$ for adherends in plane stress and $E/\left(1-\nu^2\right)$ for adherends in plane strain. G_a, c, E, t are the same variables as defined previously and h is the adhesive thickness. k is the bending moment factor as seen in Hart-Smith model. The maximum nondimensional stress at the bond/adherend interfaces is given by:

$$\tau^{**} = \tau^* \pm \Delta\tau^* \tag{12}$$

where: $\Delta\tau^* = \frac{G_a h}{2E_a}\sigma^{*'}$.

The solution for the nondimensional peel stress σ^* is given by:

$$\sigma^* = C\sinh\left(\alpha_1 x^*\right)\sin\left(\alpha_2 x^*\right) + D\cosh\left(\alpha_1 x^*\right)\cos\left(\alpha_2 x^*\right) \tag{13}$$

where $\alpha_1^2 = \frac{3\beta\lambda^2}{2} + \frac{\rho}{2}$; $\alpha_2^2 = -\frac{3\beta\lambda^2}{2} + \frac{\rho}{2}$ and $\rho^2 = \frac{24E_a c^4}{E^* h t^3}$

Constants *C* and *D* are obtained upon substitution of the derivatives of Eq. (13) into Eqs. (14) and (15)

$$\sigma^{*'''}(\pm 1) - 6\beta\lambda^2\sigma^{*'}(\pm 1) = \mp k\gamma\rho^2(1+\beta) \tag{14}$$

$$\sigma^{*''}(\pm 1) = k\gamma\rho^2(1+\beta) \tag{15}$$

where $\gamma = {}^{t}\!/_{2c}$. All analysis was done in a nondimensional basis. Equivalence is given by: $\tau^* = \frac{\tau}{\overline{\tau}}$, $\sigma^* = \frac{\sigma}{\overline{\tau}}$, $x^* = \frac{x}{c}$, where $\overline{\tau} = \frac{\overline{P}}{2c}$.

2.2. DOUBLERS

The formulation presented in this paper is referred to doublers with two layers. However, this formulation can be applied to most doublers configurations. For simplicity, were have done some considerations, as considering similar adherends and isotropic materials. Details of the method could be understood by revising the classic laminated theory.

2.2.1. C.N. DUONG

2.2.1.1. Solution for nonlinear moment distribution along the joint

The equations governing the adhesive stresses require knowledge of the bending moment at the ends of the overlap as boundary conditions. Due to symmetry, only half of the doubler configuration will be considered, as shown in Fig.1.

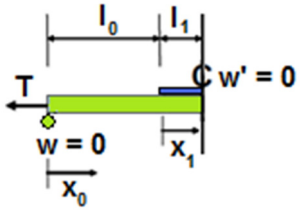

Figure 1. Schematic representation of a tapered doubler for calculating the nonlinear bending moment distribution.

From moment equilibrium consideration, the moment distribution in each segment along the joint is related to loads and displacements by:

$$M_i = -T\hat{w}_i - T\left(e_i - e_0\right) \tag{16}$$

where $i = 0, \ldots, N$; N is the number of segments (steps) in the overlapped region; segment 0 (which corresponds to $i = 0$) is outside the overlap and consists of only the bottom adherend, M is the bending moment, T is the axial tensile load applied at the ends of the adherends, $\hat{w}$ is the transverse deflection, e_i is the z-coordinate of the neutral axis of a beam cross section of the segment i measured from the bottom surface of the bottom adherend. For a homogeneous and isotropic segment:

$$e_i = \frac{T_i}{2} \tag{17}$$

$$M_i = -D_i \hat{w}_i''(x_i) \tag{18}$$

where D_i is the bending stiffness as defined previously. t_i is the segment thickness. Substituting Eq. (18) into Eq. (16):

$$\hat{w}_i'' - \frac{T}{D_i}\hat{w}_i = \frac{T(e_i - e_0)}{D_i} \tag{19}$$

Therefore, the solution of Eq. (19) is given by:

$$\hat{w}_i(x_i) = W_{1i}\cosh(\xi_i x_i) + W_{2i}\,\mathrm{senh}(\xi_i x_i) - (e_i - e_0) \tag{20}$$

where, $\xi_i = \sqrt{\frac{T}{D_i}}$. The boundary conditions are:

$$\begin{aligned} &\hat{w} = 0 \text{ para } x = 0, \text{ ou } \hat{w}_0 = 0 \text{ para } x_0 = 0, \text{ então } W_{10} = 0 \\ &\hat{w}'' = 0 \text{ for } x = l_0 + l_1 + \ldots + l_n \text{ or } x_N = l_N, \end{aligned} \tag{21}$$

Then:

$$\xi_1 W_{11} senh(\xi_1 l_1) + \xi_1 W_{21} cosh(\xi_1 l_1) = 0 \quad (22)$$

$$W_{1i}\cosh(\xi_i l_i) + W_{2i}\sinh(\xi_i l_i) - W_{1.i+1} = e_i - e_{i+1} \quad (23)$$

$$l_i W_{1i}\,\mathrm{senh}(\xi_i l_i) + l_i W_{2i}\cosh(\xi_i l_i) - l_{i+1} W_{2,i+1} = 0 \quad (24)$$

So, the nonlinear bending moment at the end of the overlap is given be:

$$M_l = M_0(x_0 = l_o) = -\xi_0 D_0\{W_{10}\cosh(\xi_0 l_0) + W_{20}\,\mathrm{senh}(\xi_0 l_0)\} \quad (25)$$

2.2.1.2. Solutions for peel and shear stresses in the adhesive

Using their nonlinear estimate for the bending moments in the adherends just outside the bonded area from the first step rigid bond analysis as the key boundary conditions. The equilibrium equations is show in Figure 2.

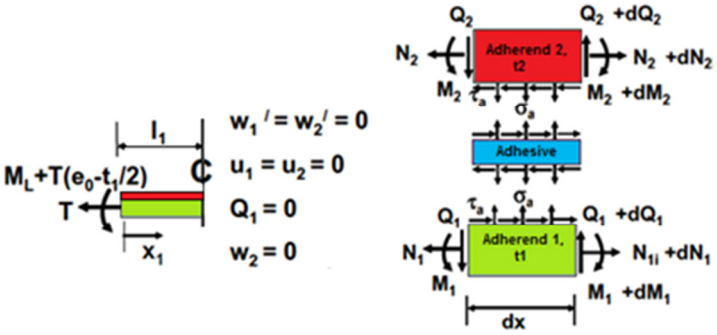

Figure 2 – Schematic diagrams for calculating adhesive peel and shear stresses.

These equilibrium equations can be written as follows:

For the bottom adherend:

$$\begin{aligned} N'_1 &= -\tau_a, \\ Q'_1 &= -\sigma_a, \\ M'_1 &= Q_1 - \tau_a\left(\frac{t_1+t_a}{2}\right) - N_1 \,.\, \hat{w}' \end{aligned} \quad (26)$$

For the doubler or upper adherend:

$$\begin{aligned} N'_2 &= -\tau_a, \\ Q'_{2i} &= \sigma_a, \\ M'_2 &= Q_2 - \tau_a\left(\frac{t_2+t_a}{2}\right) - N_2 .\, \hat{w}' \end{aligned} \quad (27)$$

where N and Q are normal stress resultant and vertical shear resultant, respectively. M again denotes the moment, σ_a and τ_a are the adhesive shear and peel stresses. t_1, t_2 and t_a are the total thickness of the bottom adherend, upper adherend, and adhesive layer, respectively. $\hat{w}$ is the transverse deflection. The subscripts 1 and 2 denote the bottom adherend and the doubler, respectively.

The effect of the geometrical nonlinearity is accounted in the present formulation by including the underlined terms in Eqs. (26) and (27). These terms represent approximately the additional moment in the adherend and doubler due to their large bending deflections. Eqs. (26) and (27) will provide a system of linear differential equations that can be solved by an appropriate numerical method.

2.2.2. HART-SMITH SOLUTION FOR DOUBLERS

Following a similar derivation as given by (Duong, 2006), the transverse displacement inside the overlap and the peak bending moment at the end of the overlap are obtained by (Hart-Smith, 2004) as:

$$\widehat{w}(x) = e\left\{1 - \frac{\cosh(\xi_1 x)}{\left[\cosh(\xi_1 c) + \left(\frac{\xi_1}{\xi_0}\right)\sinh(\xi_1 c)\right]}\right\} \tag{28}$$

$$M_0 = -\frac{\left(\frac{\xi_1}{\xi_0}\right)\tanh(\xi_1 c)}{\left[1 + \left(\frac{\xi_1}{\xi_0}\right)\tanh(\xi_1 c)\right]} T_e \tag{29}$$

where:

$$e = \frac{E_d t_d \left(\frac{t_s + t_d}{2}\right)}{E_s t_s + E_d t_d} = \frac{S}{1+S}\left(\frac{t_s + t_d}{2}\right), \quad S = \frac{E_d t_d}{E_s t_s}, \tag{30}$$

$$D_0 = \frac{E_s t_s^3}{12\,(1-\upsilon_s^2)},\; D_1 = \frac{E_s t_s^3}{12\,(1-\upsilon_s^2)} + \frac{E_d t_d^3}{12\,(1-\upsilon_d^2)} + e^2 E_s t_s + \left(\frac{t_s + t_d}{2} - e\right)^2 E_d t_d \tag{31}$$

Where *c* is the half doubler length, subscripts *s* and *d* denote the skin and doubler, respectively. Coordinate *x* is measured from the doubler center and the rest are defined similarly as in (Duong, 2006).

Once the bending moment and the transverse displacement are calculated, the peel and shear stresses in the adhesive can be determined following the solution procedure given below.

Peel stress analysis:

The adhesive peel stresses can be expressed by the differential transverse deflection between the skin and the patch:

$$\frac{\sigma_a}{E_a} = \frac{w_s - w_d}{t_a} \tag{32}$$

And the general solution can be approximated by:

$$w_s - w_d \approx e^{-\chi s}(A\cos(\chi s) + B\sin(\chi s)) \tag{33}$$

where:

$$\chi^4 = \frac{E_a}{t_a(D_0 + D_d)}, \qquad D_d = \frac{E_d t_d^3}{12(1-\upsilon_d^2)} \tag{34}$$

and *s* is the local coordinate measured from the free edge of the doubler. With coefficients *A* and *B* defined, the peel stress is then calculated as:

$$\sigma_a = \frac{E_a}{t_a}\frac{M_0}{2\chi^2 D_0} e^{-\chi s}\{\cos(\chi s) - \sin(\chi s)\} \tag{35}$$

Shear stress analysis:

In contrast, adhesive shear strains and stresses can be established by the differential longitudinal displacements *u*, between the skin and the patch:

$$\gamma_a = \frac{\tau_a}{G_a} = \frac{u_s - u_d}{t_a} \tag{36}$$

The governing equation for the shear stress have the following form:

$$\frac{d^3\tau_a}{dx^3} = 4\lambda^2 \frac{d\tau_a}{dx} \tag{37}$$

where:

$$\lambda^2 = \frac{G_a}{t_a}\left(\frac{1}{E_s t_s} + \frac{1}{E_d t_d}\right), \tag{38}$$

where the coefficients to be determined by the boundary conditions and the adhesive shear stress within the overlap can then be rewritten as following:

$$\tau_a = \frac{G_a}{2\lambda t_a E_s}\left(\frac{T}{t_s} - \frac{6M_0}{t_s^2}\right)e^{-2\lambda s} + \frac{1}{c}\left[T\left(\frac{S}{S+1}\right) - \frac{G_a}{4\lambda^2 t_a E_s}\left(\frac{T}{t_s} - \frac{6M_0}{t_s^2}\right)\right] \tag{39}$$

3. NUMERICAL COMPARISON

Most of the analytical methods exposed above considered both adherends and adhesives as been perfectly elastic. Including the non-linearity of the material turns the problem complex, and as the degree of complexity increases, the initial analytical problem must be solved numerically. This paper shows a comparison between analytical models and numerical results. For the numerical validation the commercial software ABAQUS® was used.

3.1. Single lap joints (SLJ)

Geometry was in accordance with the ASTM D1002 standard, as shown in Fig. 3. The adhesive used was the AF 163-2K.045WT from 3M Company. This adhesive has a nominal thickness of 7.5 mils (0.19mm), an Elasticity modulus of 1120 MPa and a Poisson ratio of 0.34. The adherend used was aluminum 2024-T3, which have an elasticity modulus of 73100 MPa and a Poisson ratio of 0.33. For the comparison was considered an applied load of 1000N.

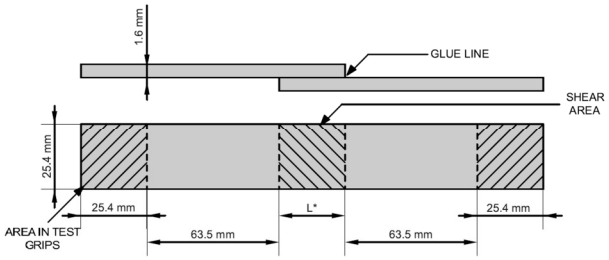

Figure 3. Form and dimensions of test specimens

For the analysis was used the 2D Abaqus element CPE8R for the adhesive and the adherends. The CPE8R is an eight – node biquadratic plane strain quadrilateral element. In sum were used 400 elements in the adhesive and 960 elements in the adherend. Results of the comparison are shown in Figure 4. Details of the mesh for both shear and peel stresses are shown in Figure 5. It is worthed to mention that numerical models were able to predict the zero shear stress at the end of the adhesive layer due to the stress-free condition at the overlap ends. With this, analytical models overestimate the stress at the ends of the overlap and tend to give conservative failure loads predictions, da Silva et al (2009). Additionaly, special care was taken into account at the overlap ends, a higher mesh refinement were reached to better describe the behaviour at this zones. To reach an optimal mesh it was accomplished a mesh refinement. This procedure was realized by increasing the number of elements at overlap ends and analyzing the maximum stress behaviour and its convergence.

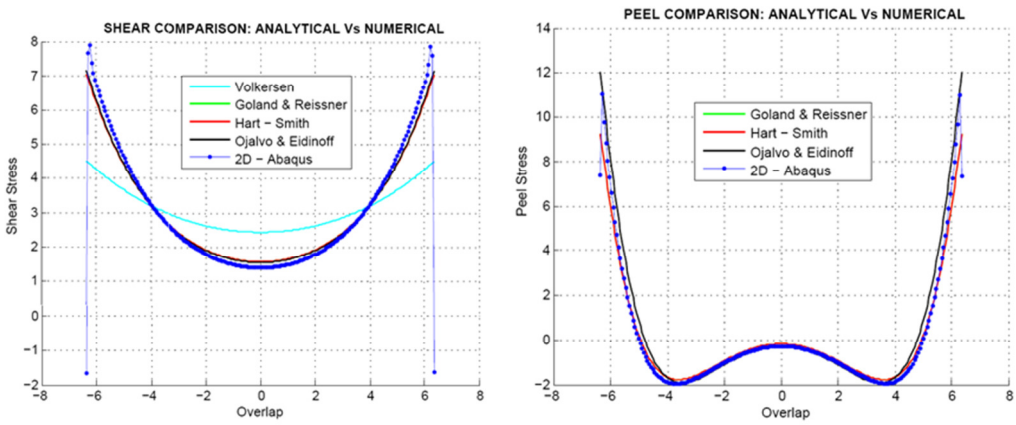

Figure 4. Shear and Peel comparison for a SLJ configuration

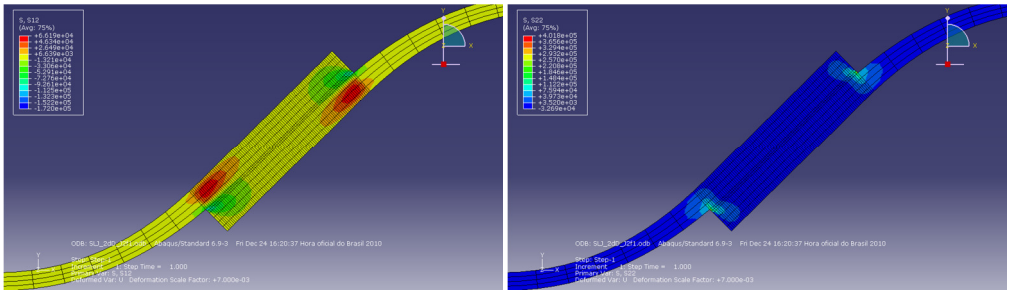

Figure 5. Mesh details for shear and peel stresses for a SLJ configuration

3.2. Doublers

The geometry (Fig. 6) and material properties of the adherends and of the adhesive are given below (with subscripts *1, 2* and *a* denoting the bottom adherend, doubler or upper adherend and adhesive, respectively):

Adherend: $E_1 = E_2 = 68950$ MPa, $\upsilon_1 = \upsilon_2 = 0.3$, $t_1 = t_2 = 1.27$ mm.
Adhesive: $E_a = 1793$ MPa, $G_a = 689.5$ MPa, $t_a = 0.127$ mm.
Tensile load and Geometry : $T/t_1 = 137.9$ MPa, $l_0 = 254$ mm, $l_1 = 63.5$ mm.

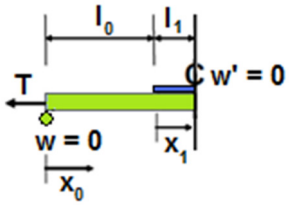

Figure 6. Schematic representation of a tapered doubler in example.

Again, for the numerical analysis was used the 2D Abaqus element CPS8R for the adhesive and the adherends. Results of the comparison are shown in Fig. 8. Details of the mesh and Von-Mises stress for doubler and adhesive are shown in Fig. 7.

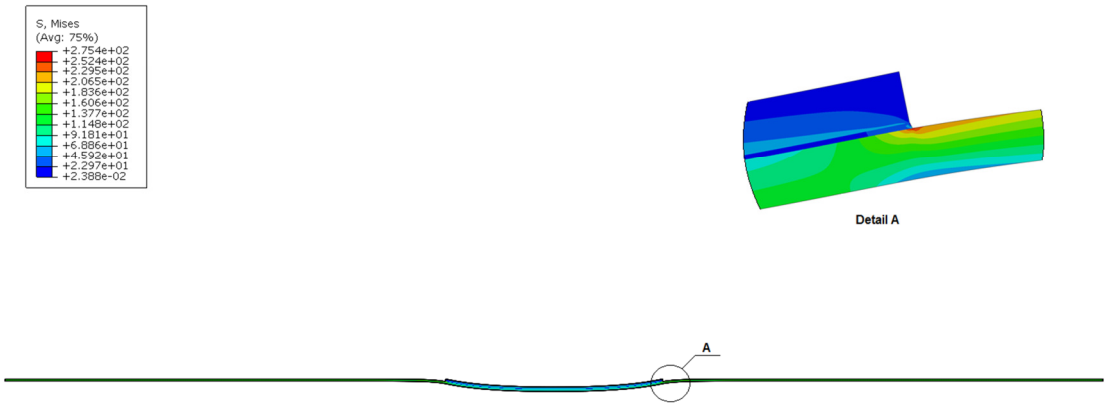

Figure 7. Details and Von-Mises stress for doubler and adhesive.

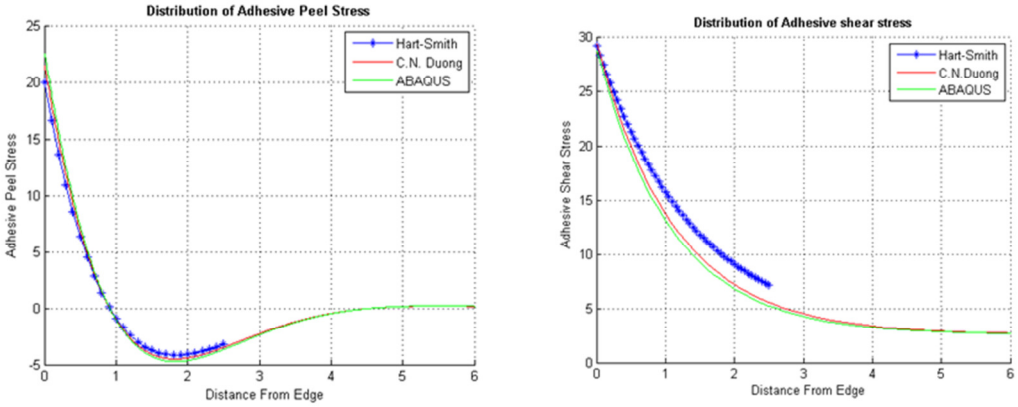

Figure 8. Shear and Peel comparison.

4. CONCLUSIONS

This paper shows several analytical models for both SLJ and doubler configurations. For the validation of analytical methods implemented were used the finite element method (FEM) by the use of the commercial software ABAQUS ®. Results achieved showed concordance with the literature. A more extensive review of the SLJ configuration was done by (Rodríguez et al., 2011) and their paper could be considered as complementary to the present work.

A Doubler represents a structure that involves two substrates and a thin adhesive layer, the stress states that exist at various levels in a bonded doubler are very complex. Consequently, some theories exist to estimate analitically stress distributions for bonded doublers. These theories are essentially based on the work of (Hart-Smith, 1973; 2004) and (Duong, 2006). Using the relatively simple theory of (Hart-Smith, 2004), explicit solutions can be derived and all features of prime importance can be studied. However, the theory of Hart-Smith doesn't consider the coupling effect between peel and shear in an unbalanced doubler. This effect is shown in (Duong, 2006) work, this fact is a major reason for the proximity between analytical and numerical curves, as shown in Fig. 8.

5. REFERENCES

ASTM D1002, "Standard Test Method for Apparent Shear Strength of Single-Lap-Joint Adhesively Bonded Metal Specimens by Tension Loading (Metal-to-Metal)"

Duong, C. N. A unified approach to geometrically nonlinear analysis of tapered bonded joints and doublers. International Journal of Solids and Structures, 43: 3498-3526, 2006.

Da Silva, L.F.M, das Neves, P.J.C., Adams, R.D. and Spelt, J.K. Analytical models of adhesively bonded joints – Part I: Literature survey, *International Journal of Adhesion and Adhesives*, 2009 (29), pp. 319-339.

Goland M., Reissner E., "The Stresses in Cemented Joints", *Journal of Applied Mechanics*, Vol.11, March 1944, pp. A17-A27.

Hart-Smith, L. J., "Adhesive-Bonded Single-Lap Joints", NASA CR-112236, January 1973.

Hart-Smith, L.J., 2004. Analyses of adhesive peel and shear stresses in bonded single-strap joints and one-sided patches and doublers, accounting for thermal mismatch effects, in press.

Ojalvo I.U, Eidinoff H.L., "Bond Thickness Effects upon Stresses in Single-Lap Adhesive Joints", *American Institute of Aeronautics and Astronautics Journal*, 1978, Vol.16, No 3, pp. 204:211.

Rodríguez R.Q., Sollero P., Albuquerque E.L., "Stress Analysis and Failure Criteria of Adhesive Bonded Single Lap Joints", COBEM 2011, accepted for oral presentation, 2011.

Vokersen O., "Nietkraftverteiligung in zugbeanspruchten nietverbindungen mit konstanten Laschenquerschnitten", Luftfahrtforschung, 1938, pp. 15:41.

6. RESPONSIBILITY NOTICE

The authors are the only responsible for the printed material included in this paper.